From Stardust to Planetesimals
ASP Conference Series, Vol. 122, 1997
Y.J. Pendleton and A.G.G.M. Tielens (eds.)

The Kuiper Belt

David Jewitt

Institute for Astronomy, 2680 Woodlawn Drive, Honolulu, HI 96822

Jane Luu

Harvard University, 60 Garden Street, Cambridge, MA 02138

Abstract. The region beyond Neptune contains a vast number of small solid bodies collectively known as the Kuiper Belt. They are previously unknown remnants from the accretion disk out of which the solar system formed, and may house the least thermally processed materials in the solar system. The Kuiper Belt is the probable source of the short-period comets, and a potential source of dust generated by mutual collisions.

1. Introduction: The Kuiper Belt, Plutinos and Centaurs

This review is divided into two parts. First, we discuss the basic parameters of the Kuiper Belt and allude to the significance which modern planetary science attaches to it. Second, because of the special focus of the "Stardust" meeting, we address the Kuiper Belt as a potential source of dust. A complementary review of the Kuiper Belt on a more popular level is given in Luu and Jewitt (1996).

The solar system formed about 4.6 Gyr ago from a centripetally flattened disk of mixed gas and dust. Close to the sun, refractory dust particles collided and grew into ever larger aggregates ("planetesimals"), at first as a result of being sticky, and later as a result of gravitational attraction. In the inner disk, accretion produced the familiar terrestrial planets, composed mainly of Fe, Si, O and S. Beyond heliocentric distance $R \sim 5$ AU, the disk temperatures were low enough that water could be incorporated into planetesimals as solid ice; other more volatile materials such as CO, CO_2 and various hydrocarbons may also be trapped at larger distances (lower temperatures). The resulting rock/ice agglomerates grew large enough (5 to 10 $M_\oplus$) to accrete hydrogen/helium envelopes directly from the surrounding disk, forming the gas giants, Jupiter and Saturn. Uranus and Neptune grew so slowly that their cores reached critical mass only after the bulk of the hydrogen/ helium nebula had been cleared (perhaps by a strong magnetic wind from the young sun). As a result, they lack the characteristic (near) solar compositions evident in Jupiter and Saturn. Beyond Neptune ($R > 30$ AU) the disk appears to have been of too low a density to form massive planets, although it has long been speculated that smaller objects might form (Edgeworth 1949, Kuiper 1951).

The forming gas giants were very effective in scattering planetesimals from the surrounding disk, and a great many such objects were ejected into interstellar space. The orbits of perhaps 10% of the ejected planetesimals were perturbed by nearby stars (Oort 1950), and by the gradient in the gravitational potential of the Milky Way (Heisler and Tremaine 1986) into loosely bound orbits at vast distances (tens of thousands of AUs). A swarm of perhaps 10^{12} such objects still orbit the sun to this day, and is known as the Oort Cloud (radius $\sim$ 50,000 AU). Planetesimals in the Oort Cloud occasionally diffuse back into the gravitational control of the planets, where they appear to us as the long period comets (LPCs). Their semi-major axes and orbital eccentricities are typically large. Equal numbers of prograde and retrograde LPCs are observed, showing that the Oort Cloud is spherical as a result of continued stellar perturbations.

Much closer than the Oort Cloud, the trans-Neptunian region contains a vast abundance of solid bodies (the "Kuiper Belt") that appear to have survived gravitational perturbations by Neptune (Jewitt and Luu 1993, 1995; Jewitt *et al.* 1996). These objects are believed to have undergone minimal thermal processing since formation. With blackbody equilibrium temperatures $\approx$ 40 K, water is stable as a solid over the age of the solar system, and even very volatile molecules such as CO and CO_2 can be held indefinitely (Bar-Nun *et al.* 1987). The large Kuiper Belt objects are likely to contain primitive matter that may record conditions at, or even slightly before, the epoch of planet growth. When scattered into the inner solar system by the gravitational action of the major planets, Kuiper Belt objects begin to sublimate their near-surface volatiles and are identified as short-period comets (SPCs). Roughly (1 to 10) $\times 10^9$ Kuiper Belt objects are required to supply the SPCs (Fernandez 1980, Duncan *et al.* 1988). At intermediate distances (roughly $5 \leq R \leq 30$ AU) Kuiper Belt escapees are known as Centaurs. They are characterized by short dynamical lifetimes $\approx 10^6$ to 10^7 yr, owing to scattering by the gas giants (Dones *et al.* 1996).

As of September 1996, 36 Kuiper Belt objects have been identified from ground-based observations. The sizes of these bodies are not directly measured, since their albedos are unknown. On the assumption that the geometric red albedos are similar to those measured for the nuclei of comets ($p_R \approx 0.04$), we compute representative diameters in the range $100 \leq D \leq 400$ km, much larger than the nuclei of typical short-period comets. Most likely, these objects represent the larger bodies in a size distribution that extends all the way down to the km-scales of the cometary nuclei. Unfortunately, the small bodies are faint and difficult astronomical targets, and essentially nothing is known about them with confidence.

So far, only a few square degrees of the sky have been searched for Kuiper Belt objects. An extrapolation to the full 10^4 square degree area of the ecliptic band reveals that the Belt contains about 70,000 objects larger than 100 km diameter in the $30 < R < 50$ AU region (Jewitt *et al.* 1996, hereafter JLC96). This is almost 1000 times larger than the population of comparably sized main-belt asteroids and gives an idea of the magnitude of the trans-Neptunian population. The distribution of brightnesses of the 36 ground-based objects is compatible with power-law differential size distributions $n(D)dD = \Gamma D^{-q} dD$, where D is diameter, Γ = constant and $q = 3$. The total mass of the distribution is poorly

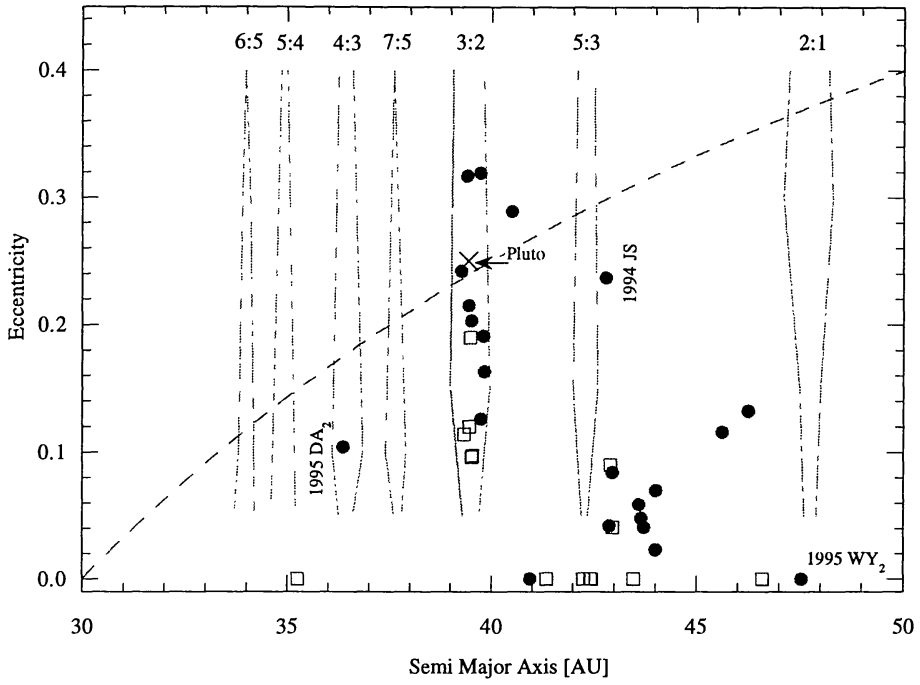

Figure 1. Semi-major axis vs. orbital eccentricity of the Kuiper Belt objects. Higher quality orbital elements computed from astrometry taken over $N > 1$ opposition (circles) are distinguished from lower quality elements determined from astrometry within the discovery year (squares). Pluto is marked with an X. Locations of mean motion resonances are marked and labelled (from Malhotra 1995). The dashed line marks perihelion distance $q = 30$ AU. Objects above the line are Neptune-crossing.

determined, but values up to $0.3M_\oplus$ are not unreasonable (JLC96). A limit of about $1M_\oplus$ has been placed from the absence of gravitational perturbations on comet Halley (Yeomans 1986, Hogg *et al.* 1991).

The orbital periods of these bodies are very long (e.g., 250 yr at 40 AU), so that the limited observations available so far permit only imperfect estimates of the orbital parameters. Nevertheless, some general orbital characteristics of the trans-Neptunians are well established. The distribution of orbital semi-major axes is highly non-uniform (Fig. 1), with a major concentration at the 3:2 mean motion resonance with Neptune (semi-major axis $a = 39.4$ AU). Fully 35% of the known Kuiper Belt objects are in this resonance, together with Pluto, which we view as the largest known Kuiper Belt object. The number of these "Plutinos" (with diameters > 100 km) is of order 30,000 (JLC96). In addition, a single object has been identified in the 4:3 resonance at $a = 36.3$ AU.

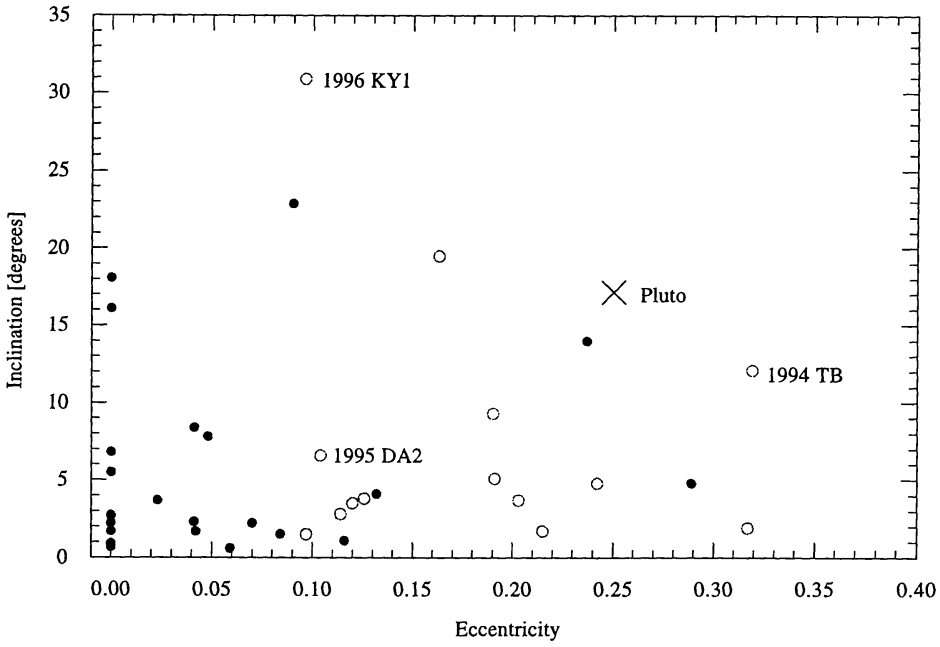

Figure 2. Orbital eccentricity vs. inclination for resonant (empty circles) and non-resonant (filled circles) Kuiper Belt objects. The resonant objects (all but 1995 DA2 are in the 3:2 resonance at 39 AU) possess systematically larger eccentricities than the non-resonant objects.

Resonant orbits presumably protect the Plutinos from close encounters with Neptune, just as Pluto is so protected. Like Pluto, four of the Plutinos (1993 SB, 1994 TB, 1995 HM5, and 1995 QY9) have perihelia inside the orbit of Neptune (Fig. 1). Plutinos with larger eccentricities (e.g., 1994 TB) and inclinations (e.g., 1996 KY1) than Pluto have already been identified. These observations show that Pluto is distinguished from its siblings mainly by its size (2200 km diameter compared with about 400 km for the largest Plutinos yet identified). They also raise the intriguing question of how so many objects could have become trapped in the resonant orbits. A promising resonant capture scenario has been developed by Malhotra (1995, 1996) following the realization that Neptune may have migrated radially as a result of angular momentum exchange with the surrounding planetesimal disk (Fernandez and Ip 1984). Collisional processes may also be implicated in both populating and depopulating the resonances (Farinella and Davis 1996).

Simulations show that resonance capture tends to pump the orbital eccentricity and inclination (Holman and Wisdom 1993, Duncan *et al.* 1995, Malhotra 1995). The eccentricities of resonant Kuiper Belt objects are indeed statistically larger than those of non-resonant objects (Fig. 2), although the case for the inclinations is less clear. Note that the ecliptic surveys discriminate against the discovery of KBOs with high inclination, and that the proportion of KBOs of high inclination is much higher than suggested by Fig. 2. On-going observations will provide critical tests of dynamical models of the Kuiper Belt.

Six Centaurs are known at the time of writing. The most famous example, 2060 Chiron, shows cometary activity at $R \approx 10$ AU (Luu and Jewitt 1990), and possibly also at 20 AU (Bus *et al.* 1989), providing direct evidence for materials more volatile than water ice. As we have noted, this is in keeping with the prior storage of Chiron at low temperatures in the Kuiper Belt. Although very few Centaurs are known, it is already apparent that there exists a discrepancy between the measured Centaur abundance (JLC96) and the only published prediction of this quantity (Irwin *et al.* 1995). The 50 times over-abundance of the Centaurs implies a population ≈ 2600 (diameters > 75 km), while the total mass flux from the Kuiper Belt through the Centaurs in the age of the solar system may have reached $\approx 1 M_\oplus$ (JLC96).

2. Collisions and Dust Production

The physical parameters of the Kuiper Belt are still quite poorly known, leading to major uncertainties in the estimated rates and significance of collisions among Kuiper Belt objects. The most rankling uncertainties pertain to the small body (kilometer scale) population, since small bodies most likely dominate the collision rate. Accordingly, we focus here on relatively robust order-of-magnitude arguments, while making reference to more detailed models based on specific assumptions about the number densities and collision rates.

The inclination and eccentricity distributions of the Kuiper Belt objects are very broad (see Fig. 2; JLC96), so that mutual collisions occur at typical velocities > 1 km/s, are predominantly erosive, and will lead to the production of dust. For example, the collisional time among bodies of radius a is of order $t_c \approx (4\pi N_1 a^2 \Delta V)^{-1}$, where N_1 is the number density of objects and ΔV is the

velocity dispersion amongst them. For illustration, we assume that the 7×10^4 QB1-class trans-Neptunians occupy a disk 10 AU thick with inner and outer edges $30 \leq R \leq 50$ AU from the sun (JLC96). With representative values $a = 100$ km and $\Delta V = 2$ km/s, we find that, for a QB1-like object, $t_c \approx 10^{19}$ s ≈ 300 Gyr. Considering all 7×10^4 objects, we estimate that mutual collisions between QB1-size objects occur on timescales ≈ 4 Myr, and that in the age of the solar system only about 10^3 such collisions (representing $\sim 1\%$ of the QB1 population) have occurred.

On the other hand, the more numerous, small (e.g. km-sized) objects, can collide with QB1's much more frequently. For example, if 1 (10) billion km-sized objects occupy the same volume, the collision time falls to $t_c \approx 7 \times 10^{14} (7 \times 10^{13})$ s $\approx 20(2)$ Myr per QB1-sized target, and among 7×10^4 such targets, the interval between impacts is a remarkably short 300 (30) years. Given a sufficiently steep size distribution, collisions between small Kuiper Belt objects might dominate over collisions with QB1s, decreasing the collision time still further. Destructive impacts between km-sized Kuiper Belt objects should create expanding debris clouds that may approach naked-eye visibility (magnitude 6) on timescales of days (Alcock and Hut 1993), and fade to invisibility over the course of several years (Stern 1995). Indeed, detection of discrete debris clouds may be the most accessible method by which to assess the small body population in the Kuiper Belt.

Escape velocity from a 100 km sized body is ≈ 0.1 km/s. Some of the ejecta from such a large target might be recaptured, leading to a "rubble pile" (as opposed to monolithic) structure for the larger Kuiper Belt objects (Farinella and Davis 1996). Conversely, the ejecta from small body collisions will be widely dispersed in the Kuiper Belt. If each km-sized impact results in the pulverization and dispersal of about one projectile mass, the order of magnitude rate of release of debris becomes $4 \times 10^2 (4 \times 10^3)$ kg s^{-1}. This estimate is conservative, since each impact will typically erode a substantial mass of the target, as well as destroying the projectile. Stern (1995) estimated the dust production rate as 10^6 kg s^{-1} to 3×10^8 kg s^{-1}. This dwarfs the 10^4 kg s^{-1} needed to sustain the Zodiacal Cloud (Whipple 1967), raising the possibility that the Kuiper Belt might supply significant amounts of dust to the inner solar system, provided this dust can survive the long journey to the inner solar system (see below; Flynn 1994; Liou *et al.* 1996).

3. Dust Loss

The fate of collisionally generated Kuiper Belt dust depends on the particle size. Very small dust grains (radii $a \ll 0.05$ μm) are scattered by the solar magnetic field via the Lorenz force, and will be widely dispersed. Slightly larger grains experience radiation pressure forces sufficient to eject them from the solar system. For initially circular orbital motion ($e = 0$) as expected in a Kuiper Belt source, all dust particles with $\beta > 0.5$ will be gravitationally unbound, and must immediately depart the solar system (here, β = radiation pressure acceleration / local solar gravitational acceleration). Common ice and mineral dielectric grains with radius $0.05 < a < 0.5$ μm have $\beta > 0.5$ (Burns *et al.* 1979) and so should be rare in the Kuiper Belt even if they are produced there in great abundance.

Larger grains will spiral from the Kuiper Belt towards the sun under the action of Poynting-Robertson and plasma-drag forces. The Poynting-Robertson time is

$$t_{pr} \approx \rho a c^2 R^2 / F_{sun}, \tag{1}$$

where $\rho \approx 10^3$ kg m^{-3} is the grain density, $c = 3 \times 10^8$ m/s is the speed of light and $F_{sun} = 1380$ W m^{-2} is the Solar Constant. At $R = 40$ AU, this approximates $t_{pr} \approx 3.5(a/1\ \mu\text{m})$ Myr, for particle radii measured in μm.

The characteristic timescale for plasma drag to deplete Kuiper Belt dust is

$$t_{PD} \approx \rho a / (N_1 V_{SW} m_p), \tag{2}$$

where $N_1 \approx 10^6 R^{-2}$ [m^{-3}] is the solar wind number density at distance R [AU], $V_{SW} \approx 500$ km/s is the solar wind speed, and $m_p = 1.67 \times 10^{-27}$ kg is the mass of the proton. At $R = 40$ AU, this approximates $t_{PD} \approx 63(a/1\ \mu\text{m})$ Myr, for particle radii measured in μm, or $t_{PD} \approx 20 t_{pr}$. Plasma drag is thus a less effective dust depletion process than Poynting-Robertson drag, at least under the present-day solar wind conditions.

Besides the dynamical loss processes mentioned above, dust grains may also be eroded and destroyed by collisions with interstellar grains, or with other particles in the Kuiper Belt. Collisions with interstellar grains are especially important, as they occur at high velocity and are very capable of destroying dust particles many times their own size. Specifically, impacts with interstellar grains of radius a_i will shatter dust particles up to a maximum size determined by

$$a_{max} = K a_i \tag{3}$$

with

$$K = \left(\frac{V^2}{2E_R}\right)^{1/3} \tag{4}$$

Here, $V = 26$ km/s is the incident velocity of the interstellar dust (Baghul *et al.* 1995), and $E_R = 500$ J kg^{-1} is the experimentally determined specific rupture energy (Gault and Wedekind 1969). Substitution into Eq. (4) gives $K \approx 88$. For example, interstellar grains of radius $a_{min} = 0.6$ μm are capable of shattering Kuiper Belt particles up to radius $a_{max} \approx 53$ μm.

Interpretation of the classical extinction curve for interstellar dust suggests a differential particle size distribution $n(a_i)da_i = \Gamma a_i^{-\gamma} da_i$, with $\gamma = 3.5$ in the size range $0.025 \leq a_i \leq 0.25$ μm (Mathis *et al.* 1977). The distribution for particles larger than 0.25 μm is uncertain, because large grains contribute relatively little to the total extinction cross-section. Kim *et al.* (1994) find an exponential decrease above characteristic radius $a_0 \approx 0.25$ μm, such that $n(a_i)da_i = \Gamma a_i^{-\gamma} \exp(-a_i/a_0) da_i$. On the other hand, Rowan-Robinson (1992) claims that 30- μm particles are needed to supply the submillimeter flux densities observed from the disks of galaxies. The recently reported detection of interstellar meteors (Taylor *et al.* 1996) strongly suggests that the size distribution extends up to at least 40 μm. Such large particles might be ejected

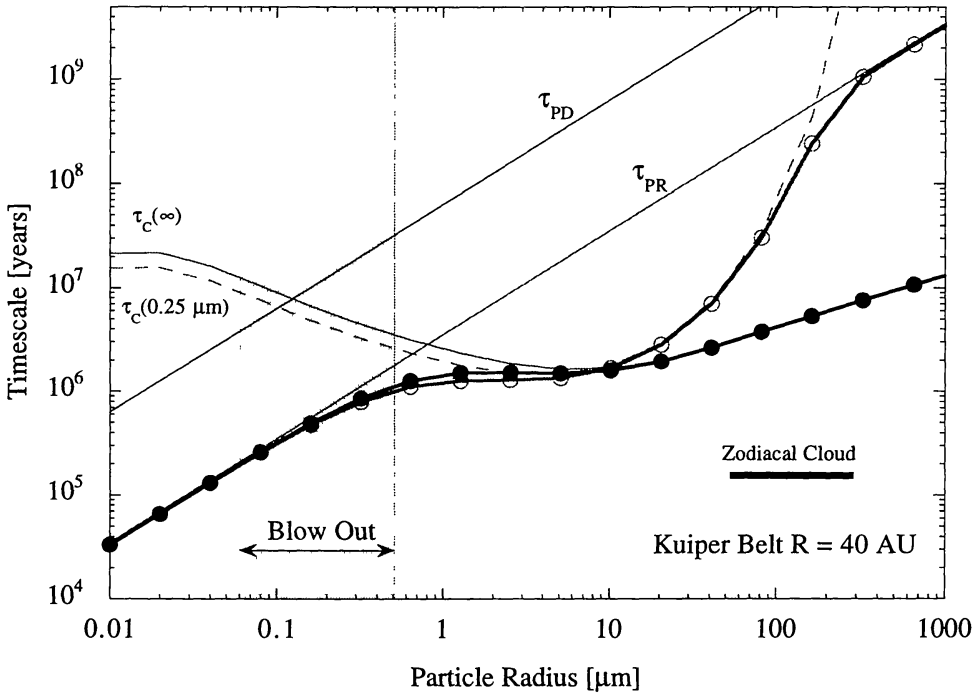

Figure 3. Timescales for Poynting-Robertson decay (t_{pr}), plasma drag (t_{pd}), and collision with interstellar dust (t_c), all plotted as a function of radius for particles at 40 AU in the Kuiper Belt. The shaded region marks particles likely to be ejected from the solar system by radiation pressure. The lines with circles show the lifetimes to all three processes combined: the line with filled circles corresponds to $a_0 = \infty$, and that with empty circles $a_0 = 0.25$ μm.

from circumstellar disks along with other macroscopic debris (including comets bound for the Oort Cloud), during the late stages of planet formation. Near the Sun, the smallest grains will be depleted relative to the interstellar distribution due to scattering by the solar magnetic field (Baghul *et al.* 1995). Indeed, the interstellar dust flux measured by the Ulysses spacecraft, $f \approx 8 \times 10^{-5}$ m^{-2} s^{-1} (Grün *et al.* 1994), was found to have a characteristic particle radius 0.6 μm (density 10^3 kg m^{-3} assumed). To satisfy these considerations, we write the interstellar dust size distribution as

$$n(a_i)da_i = \Gamma a_i^{-\gamma} \exp(-\frac{a}{a_0})\{1 - \exp(-\frac{a}{a_{min}})\} \quad (5)$$

with $\gamma = 3.5$ (Mathis *et al.* 1977) and the magnetic cut-off radius is near $a_{min} = 0.6$ μm (Grün *et al.* 1994). The constant, Γ, is determined by normalization to the Ulysses measurement of the interstellar dust flux. To gauge the effects of uncertainty at the large particle end of the size distribution, we calculate two models assuming $a_0 = 0.25$ μm (Kim *et al.* 1994) and $a_0 = \infty$.

The rate of destructive collisions onto a grain of radius a is given by

$$\frac{1}{t_C} = \int_{a/K}^{\infty} f(a_i)\pi(a + a_i)^2 da_i \quad (6)$$

Fig. 3 shows the collision timescales as a function of radius for the processes outlined above and for heliocentric distance $R = 40$ AU. The bottom two curves in Fig. 3 show the total grain lifetime computed from $t^{-1} = t_{pr}^{-1} + t_{pd}^{-1} + t_c^{-1}$. The shaded region identifies the particles which are likely to have $\beta > 0.5$, and so which will be immediately ejected from the solar system by radiation pressure.

The mass distribution in the Zodiacal Cloud is dominated by particles with mass $10^{-9} \leq m \leq 10^{-7}$ kg (Grün *et al.* 1985), corresponding to radii $60 \leq a \leq 300$ μm. These grains have collisional lifetimes ($\approx 10^7$ yr ; Fig. 3) that are comparable to transport times from the Kuiper Belt to the inner solar system ($10^{6.5}$ to $10^{7.5}$ yr: Liou *et al.* 1996). In this sense, the Kuiper Belt is potentially a source of the mass-dominant $60 \leq a \leq 300$ μm particles in the Zodiacal Cloud. Smaller particles (e.g., $1 \leq a \leq 10$ μm) are destroyed by collisions with the ISM grains on timescales $\approx 10^6$ yr, and presumably do not survive the journey to the inner solar system. The dynamical transport of small grains from the Kuiper Belt has been explored by Liou *et al.* (1996).

4. Other Kuiper Belts?

The recognition of our own Kuiper Belt leads us naturally to suspect that similar planetesimal structures might exist around other stars. Observations of infrared and submillimeter excesses show that dust is indeed common around main-sequence stars of late spectral type, e.g., β Pic and Vega (Backman *et al.* 1995, Sylvester *et al.* 1996). Dust in the β Pic disk is depleted by radiation drag and collisional destruction on timescales that are probably short compared to the lifetime of the star (however, note that the age of β Pic is a subject of debate). It must be continually replenished to maintain steady state (Harper *et al.* 1984), perhaps by collisional grinding in a Kuiper Belt. Backman *et al.* (1995) calculated that our own Kuiper Belt has a fractional bolometric luminosity (L_{dust}/L_{star})

about 10^{-2} and 10^{-4} times the values for the Vega and β Pic dust, respectively. Unfortunately, given the uncertainties concerning the Kuiper Belt size distribution (and hence the dust production rate), these estimates are necessarily model-dependent. An actual measurement of the amount of dust in the Kuiper Belt is a challenge for the next generation of infrared detectors, and may help settle the issue of Kuiper Belts around other stars.

Acknowledgments. D. Jewitt and J. Luu would like to thank NASA's Origins of Solar Systems program for support of this work.

References

Alcock, C., and Hut, P. 1993, "Comet Collisions in the Kuiper Belt"

Backman, D. E., Dasgupta, A., and Stencel, R. E. 1995, ApJ, 450, L35

Baguhl, M. *et al.* 1995, Science, 268, 1016

Bar-Nun, A., Dror, J., Kochavi, E., and Laufer, D. 1987, Phys.Rev.B, 35, 2427

Burns, J., Lamy, P., and Soter, S. 1979, Icarus, 40, 1

Bus, S., Bowell, E., Harris, A., and Hewitt, A. 1989, Icarus, 77, 223

Dones, L., Levison, H., and Duncan, M. 1996, in *Completing the Inventory of the Solar System*, eds. T. W. Rettig and J. M. Hahn, A. S. P. Conference Series, Volume 107, San Francisco, pp. 223

Duncan, M., Quinn, T., and Tremaine, S. 1988, ApJ, 328, L69

Duncan, M., Levison, H., and Budd, S. 1995, AJ, 110, 3073

Edgeworth, K. E. 1949, Mon. Not. Roy. Astr. Soc., 109, 600

Fernandez, J. A. 1980, Mon. Not. Roy. Astr. Soc., 192, 481

Farinella, P., and Davis, D. R. 1996, Science, 273, 938

Fernandez, J. A. and Ip, W.-H. 1984, Icarus, 58, 109

Flynn, G. J. 1994, LPSC XXV, 379-380 (abstract)

Gault, D. E., and Wedekind, J.A. 1969, Journal Geo. Res., 74, 6780

Grün, E., Zook, H. A., Fechtig, H., Giese, R. H. 1985, Icarus, 62, 244

Grün, E., Gustafson, E., Mann, I., Baguhl, M., Morfill, G. E., Staubach, P., Taylor, A., Zook, H. A. 1994, A&A, 286, 915

Harper, D. A., Loewenstein, R. F., Davidson, J. A. 1984, ApJ, 285, 808

Heisler, J., and Tremaine, S. 1986, Icarus, 65, 13

Hogg, D. W., Quinlan, G. D., and Tremaine, S. 1991, AJ, 101, 2274

Holman, M., and Wisdom, J. 1993, AJ, 105, 1987

Irwin, M., Tremaine, S., and Zytkow, A. N. 1995, AJ, 110, 3082

Jewitt, D. C. 1991, in *Comets in the Post-Halley Era*, eds. R. Newburn, M. Neugebauer, and J. Rahe, Kluwer Academic Publishers, Netherlands, pp. 19

Jewitt, D. C., and Luu, J. X. 1993, Nature, 362, 730

Jewitt, D. C., and Luu, J. X. 1995, AJ, 109, 1867

Jewitt, D. C., Luu, J. X., and Chen, J. 1996, AJ, 112, 1225

Kim, S.-H., Martin, P. G., and Hendry, P. D. 1994, ApJ, 422, 164

Kuiper, G. P. 1951, In *Astrophysics*, ed. J. A. Hynek, New York, McGraw-Hill, pp. 357

Liou, J.-C., Zook, H. A., and Dermott, S. F. 1996, Icarus, in press

Luu, J., and Jewitt, D. 1990, AJ, 100, 913

Luu, J. 1994, in *Asteroids, Comets, Meteors 1993*, eds. A. Milani, M. Di Martino, and A. Cellino, Kluwer, Dordrecht, pp. 31

Luu, J., and Jewitt, D. 1996, Scientific American, 274, 32

Malhotra, R. 1995, AJ, 110, 420

Malhotra, R. 1996, AJ, 111, 504

Mathis, J. S., Rumpl, W., and Nordsieck, K. H. 1977, ApJ, 217, 425

Oort, J. H. 1950, Bull. Astr. Inst. Netherlands, 11, 91

Rowan-Robinson, M. 1992, MNRAS, 258, 787

Stern, S. A. 1995, AJ, 110, 856

Sylvester, R. J., Skinner, C. J., Barlow, M. J., Mannings, V. 1996, MNRAS, 279, 915

Taylor, A. D., Baggaley, W. J., and Steel, D. I. 1996, Nature, 380, 323

Whipple, F. L. 1967, in *The Zodiacal Light and the Interplanetary Medium*, ed. J. L. Weinberg, NASA SP-150, Washington DC., pp. 409

Yeomans, D. K. 1986, Proc. 20th ESLAB Symp., ESA SP-250, Heidelberg, pp. 419